KFKI-1981-26

Z. SZŐKEFALVI-NAGY
I. DEMETER
L. VARGA
K. HOLLÓS-NAGY
L. KESZTHELYI

ELEMENTAL ANALYSIS OF SAMPLES OF BIOLOGICAL ORIGIN RELATIVE TO THEIR PROTEIN CONTENT BY MEANS OF CHARGED PARTICLE BOMBARDMENT

Hungarian Academy of Sciences

CENTRAL
RESEARCH
INSTITUTE FOR
PHYSICS

BUDAPEST

KFKI-1981-26

ELEMENTAL ANALYSIS OF SAMPLES OF BIOLOGICAL ORIGIN RELATIVE TO THEIR PROTEIN CONTENT BY MEANS OF CHARGED PARTICLE BOMBARDMENT

Z. SZŐKEFALVI-NAGY*, I. DEMETER*, L. VARGA*,
K. HOLLÓS-NAGY** AND L. KESZTHELYI*,**

*Central Research Institute for Physics,
H-1525 Budapest 114, P.O.B. 49, Hungary

**Biological Research Centre,
H-6701 Szeged, Hungary

Submitted to Analytical Biochemistry

HU ISSN 0368 5330
ISBN 963 371 803 1

ABSTRACT

The particle excited X-ray emission /PIXE/ and the $^{14}N/d,p/^{15}N$ nuclear reaction is combined for simultaneous elemental composition and nitrogen content determination in biological samples. Using the correlation between nitrogen and proton content the elemental composition is related to the protein content of the sample. The principles and main characteristics of the method are described and illustrative applications are also given.

АННОТАЦИЯ

С помощью ядерной реакции $^{14}N/d,p/^{15}N$ и ренгеновского излучения, возбужденного заряженными частицами, были одновременно измерены содержание азота и элементарный состав биологических образцов. Используя зависимость содержания азота от содержания белка удалось определить элементарный состав относительно содержания белка образцов. Показаны метод измерения, главные характеристики метода, а также некоторые возможности использования.

KIVONAT

A töltött részecskék keltette röntgensugárzás és a $^{14}N/d,p/^{15}N$ magreakció felhasználásával egyidejüleg mértük biológiai minták elemösszetételét és nitrogéntartalmát. A nitrogéntartalom és a fehérjetartalom közötti összefüggés felhasználásával lehetővé vált, hogy az elemösszetételt a minták fehérjetartalmára vonatkoztassuk. A dolgozatban ismertetjük a módszer elvét, főbb jellemzőit és néhány alkalmazást is bemutatunk.

Introduction

Elemental analysis is an important branch of analytical chemistry. In addition to chemical methods physical ones also play a significant role. Among other methods, characteristic X-rays excited by photons or charged particles have been extensively used for analytical purposes [1,2]. Both types of excitations have their own advantages and drawbacks. The charged particle induced X-ray emission /PIXE/ method is certainly superior to that of X-ray fluorescence /XRF/ as far as the quantity of material necessary for the analysis is concerned. A few micrograms of material are usually sufficient compared with milligrams required for XRF analysis. Because in biochemistry often only a small amount of material is available, PIXE is well suited for analytical biochemistry. On the other hand it needs an accelerator to provide the energetic charged particles. 'Charged particle' means protons, deuterons, alphas or heavy ions but no electrons; the last of these are used in electron microscopes equipped with Si/Li/ X-ray detectors. These intruments are widely used as microprobes [3] to determine the spatial distribution of different elements but because of the rather high background due to the bremsstrahlung of the electrons the sensitivity is orders of magnitude worse /~100ppm/ compared with the ppm range characteristic of proton excitation.

The principle of the PIXE method is to ionize the atoms of the sample by bombardment with an energetic ion beam. During the electron--rearrangement processes characteristic X-rays can be observed by suitable detectors, generally by Si/Li/ semiconductor detectors of high resolution [4]. From the intensity of the X-rays the number of emitting atoms in the bombarded volume can be calculated.

For samples of biological origin, however, very often the comparison between their elemental composition and their protein content is the most important quantity. One branch of the protein determination methods is based on the measurement of the nitrogen content in the sample and certain factors are used to convert this item of data to protein content [5].

Because of the low energy of nitrogen X-rays PIXE is not suitable for measuring nitrogen under usual experimental conditions. Even so, charged particle bombardment offers another possibility for nitrogen determination by means of nuclear reactions [6] . For this purpose the $^{14}N/d,p/^{15}N$ nuclear reaction was chosen. Because of the highly exoergic character of this reaction the kinetic energy of the backwards emitted protons leading to the ground state of the ^{15}N nucleus is nearly 10 MeV and by means of a suitable detecting system this group of protons can easily be separated from the particles from other nuclear reactions. Moreover the energetic deuterons also excite characteristic X-rays, so simultaneous PIXE analyses can be performed to determine the lighter elements /P,S,Cl,K and Ca/ present in the sample. The number of X-rays from heavier minor constituents is too low under these bombarding conditions. But, by subsequent proton irradiation, complete elemental analysis can be carried out and doubly measured light element concentrations allow the possibility of normalizing these two different kinds of measurements. This paper is devoted to describing our nuclear analytical method which combines PIXE and a nuclear reaction to perform elemental analysis of samples of biological origin relative to their protein content /PIXE-RP/.

In the next two sections the principles and main features of PIXE and the nuclear reaction methods are summarized, in the fourth part the experimental details, in the fifth part illustrative applications are given.

Characteristics of particle induced X-ray emission analysis /PIXE/.

Only the main features of the PIXE method will be summarized here, detailed discussions are available in recent reviews [1,2]. The fast ions /protons, deuterons or alphas/ produce inner shell vacancies in the bombarded atoms with considerably high cross-section, σ_i . To fill these vacancies rearrangement of the atomic electrons takes place accompanied by X-ray or Auger-electron emission as two competing processes. The cross-section for X-ray production can be expressed as

$$\sigma_p = \sigma_i \omega \qquad /1/$$

where ω is the so-called fluorescence yield defined for an atomic shell or subshell as the probability that a vacancy in that shell or subshell is filled through a radiative transition. This parameter depends on the transition involved but is nearly independent of the ionization mode. Its value for the K shell increases with the atomic number Z approximately

$$\omega = (1+\alpha Z^{-m})^{-1}$$

where $m \sim 3.4$ and $\alpha \sim 1.1 \times 10^{-5}$ [7] .

According to detailed experimental and theoretical investigations [1,2,8] , protons of 2–4 MeV energy are the optimal choice for analytical purposes. A collection of experimental K and L shell ionization cross-sections obtained by proton bombarding is plotted in Fig.1 taken from ref. [1] . In the figure u_i /i=K or L/ means the electron binding energy in the K or L shell, E is the proton energy and λ the ratio of the proton mass to the electron mass. The solid lines are the semiempirical functions developed by Johansson and Johansson [1] :

$$\sigma_i u_i^2 = \exp\left\{\sum_{n=0}^{5} b_n x^n\right\} \qquad /2/$$

where $x = \log /E/\lambda u_i /$ and the b_n coefficients are tabulated for the K and L shells in ref. [1] . The binding energy and the proton energy are measured in eV, the cross-sections are obtained in 10^{-14} cm² units. These semiempirical curves estimate the cross-sections to within an accuracy of a few per cent.

For deuteron bombardment, experimental results are very scarce [9,10]. According to the Born approximation projectiles of the same electric charge and velocity have the same ionization cross-section for a given element. As a consequence of this statement the following relation holds for protons and deuterons

$$\sigma_i (E)_{\text{deuteron}} = \sigma_i (E/2)_{\text{proton}} \qquad /3/$$

Most recent X-ray production cross-section measurements confirm this relation for P,S,Cl,K,Ni,Cu and Ga in the deuteron energy range of 1.6-4.0 MeV [10] . Figure 2 shows the production cross-sections of K and L X-rays vs. X-ray energies induced by proton bombardment of 2 MeV energy. The curves are calculated by equations /1/ and /2/. /The curve for L X-rays is quite illustrative because the L shell consists of three subshells resulting in a group or different L radiations even though the total cross-section values are plotted at the specific L_{α_1} X-ray energies./ Above the X-axis different elements are indicated at the energies of their K radiation; below the axis the same is done for L_{α_1} radiation. Figure 2 also shows the efficiency curve for a commercial Si/Li/ X-ray detector having a 2.5×10^{-3} cm thick Be window /1 mil /.From the figure it can be seen that for the determination of elements having an atomic number between 13 and 47 /from Al to Ag/ the K X-rays, and for heavier elements the L X-rays are convenient.

In the case of thin targets /a target can be considered as a thin one when its surface density is smaller than 1 mg/cm² [1] / the number of detected X-rays is given as

$$N_x = \frac{\Omega}{4\pi} n N_p \sigma_i \omega \eta \qquad /4/$$

where n is the number of atoms of interest per cm² of target, N_p the number of projectiles hitting the target, σ_i the ionization cross-section of the shell considered, ω the fluorescence yield, Ω the solid angle of the detector and η is the detection efficiency including all absorption effects.

However, in most practical cases the targets tend to be thick, so when calculating the X-ray yield the slowing-down of the bombarding particles and the absorption of X-rays in the target itself must be taken into account. In this case we have to use the so-called thick target yield formula [2] :

$$N_x = \frac{\Omega}{4\pi} N_p \eta c \frac{N}{A} \omega \int_{E_p}^{E_o} \sigma_i(E) \frac{dE}{S(E)} e^{-\bar{\mu}\bar{x}(E)} \qquad /5/$$

where the new symbols c,A,N mean concentration, the atomic weight of the element of interest, and the Avogadro number, respectively. S/E/ is the stopping power of the target material characterizing the slowing-down of the projectile, $\bar{\mu}\bar{x}$ symbolizes the linear attenuation factor of the outgoing X-rays in the target itself:

$$\bar{\mu}\bar{x}(E) = \bar{\mu} \int_{E_p}^{E} \frac{dE}{S(E)} \frac{\cos\theta_i}{\cos\theta_o}$$

where θ_i and θ_o are the angle of incidence of the particle trajectory and that of the emitted X-rays. In usual experimental conditions $\theta_i = \theta_o$, $\bar{\mu}$ is the average mass attenuation coefficient of the sample. For biological samples $\bar{\mu}$ is assumed to be equal to the arithmetic mean of the mass attenuation coefficients of oxygen and carbon tabulated in several compilations [11] . The stopping power values are also available from tables [12] , but Folkmann [8] developed an analytical expression for protons which approximates rather well the tabulated values:

$$S(E) = -Z^{-0.33} E^{-0.7} \cdot 0.425 \frac{\text{MeV cm}^2}{\text{mg}} \qquad /6/$$

where Z is the atomic number of the target material, and E is measured in MeV.

This equation may be more convenient for evaluating the integral in equation /5/. For composite targets an effective Z^{eff} has to be used, which is given as

$$(Z^{eff})^{-0.33} = \sum_i p_i Z_i^{-0.33} \qquad /7/$$

where p_i is the weight proportion of the i-th constituent with atomic

weight A_i and stoichiometric coefficients c_i /$p_i = c_i A_i / \sum_j c_j A_j$/ . In the derivation of equation /7/ Bragg's rule for the energy loss cross-sections was used [6] . To calculate the deuteron stopping powers a relation similar to equation /3/ can be used:

$$S(E)^{\text{deuteron}} = S(E/2)^{\text{proton}}$$

A typical proton excited X-ray spectrum of biological material is shown in Fig.3. In addition to the well resolved characteristic X-ray peaks, the smoothly curved continuous background contribution is clearly present. This radiation comes mainly from the bremsstrahlung of the projectiles, from the bremsstrahlung of the secondary electrons / δ-electrons/ emitted from the target and from Compton scattering of high energy γ -rays originating from possible nuclear reactions. Generally the second process gives the dominant part of the background and determines the characteristic decreasing shape of it vs. proton energy. /The low-energy cut-off of the spectrum is due to the rapidly increasing absorption of the detecting system./ The contribution from the nuclear reaction strongly depends on the composition of the sample and on the bombarding particle. In the case of proton bombardment by biological materials this contribution is negligible; by deuteron bombardment, however, a small but constant background shows up in the higher energy range.

The behaviour of the production cross-sections, the magnitude of the background and the efficiency of the detector system all together determine the overall sensitivity of the PIXE method. One way to express the sensitivity is to give the minimum detectable amount of the element of interest. According to statistical considerations a peak in the spectrum is said to be detectable when the number of the pulses satisfies the relation

$$N_x \geq 3\sqrt{N_B}$$

where N_B is the number of background pulses in the same energy interval. The background, however, depends on the composition of the sample; no general expression for the sensitivity can be given. Because biological

materials are mainly composed of light elements /hydrogen, carbon, nitrogen, oxygen/, the sensitivity curves calculated for a thick carbon matrix can be used as satisfactory guides /Fig.4/. These curves were calculated on the basis of refs. [1] and [8] . From the figure it can be seen that the sensitivity tends to be uniform for all elements heavier than Na; for the important trace elements /Fe,Cu,Zn,...../ it is in the ppm range. In addition to rapidity and the multielemental nature of PIXE this nearly uniform sensitivity is one of the principal reasons for utilizing this method. When calculating the smooth sensitivity curve the effects of possible interferences /for example, K K_α and Cd L_β , or As K_α and Pb L_{α_1} peaks/ were not taken into account: special care must be taken to resolve these interferences.

Summarizing, PIXE is fast, multielemental, highly sensitive, non--destructive analytical method capable of analysing a very small amount of material.

Analysis by nuclear reactions

By bombarding a target with fast ions nuclear reactions can occur between the projectiles and nuclei present in the sample. The most frequent two body reaction can be symbolized as

$$a + A \longrightarrow B + b \qquad \text{or} \qquad A/a,b/B$$

where A is the target nucleus supposed as being at rest, a is the projectile, b and B are the light and the heavy reaction product, respectively. Generally the b particles, which can also be photons, are detected. In the following, light reaction products are supposed as being charged particles. In a nuclear reaction the total energy and momentum are conserved, kinematic relations could be derived using these conserved quantities [6] . A nuclear reaction can be characterized by its Q-value which is the internal energy difference of the initial and final configurations:

$$Q = /m_a + m_A - m_b - m_B/c^2$$

where m_i is the mass of the neutral atom i. If $Q > 0$, kinetic energy is gained and the reaction is said to be exoergic. When $Q < 0$, the reaction is called to be endoergic and to produce the reaction the bombarding energy must exceed a certain threshold energy being always greater than $|Q|$. The kinetic energy of the light reaction product flying out at an angle φ with respect to the bombarding beam direction in the laboratory frame of reference can be expressed as [6]

$$E_b^{1/2} = \frac{(m_a m_b E_a)^{1/2}\cos\varphi}{m_b + m_B} \pm \frac{\{m_a m_b E_a \cos^2\varphi + (m_B + m_b)[m_B Q + (m_B - m_a)E_a]\}^{1/2}}{m_b + m_B} \qquad /8/$$

where E_a is the laboratory energy of the projectile.

From equation /8/ it can be seen that in contrast to the PIXE case the energy of the detected reaction product depends on the bombarding energy and detecting angle as well, in addition to the reaction mechanism involved. The cross-section for a certain nuclear reaction also varies with the projectile energy: it can behave smoothly or can show resonances, no general form for the energy dependence can be given. Experimental investigations are needed for each particular reaction. The cross-section of different nuclear reactions are orders of magnitude lower compared with X-ray production cross-sections and seldom exceed one barn /1 barn = $= 10^{-24}$ cm^2/. Furthermore, in a given nuclear reaction only one isotope of the element of interest takes place. In addition to the concentration of this element the abundance of the specific isotope also influences the yield of the given nuclear reaction. To determine the energy spectrum of the light reaction product b, the slowing-down in the sample must be also considered. The geometrical situation in an actual measurement is shown in Fig.5. The bombarding particle a strikes the target surface with its original energy E_a. Let us assume that the reaction takes place at depth x where the particle has reduced energy E'_a. The energy loss is determined by the stopping power $S_a/E/$ of the target material for particles of type a. The probability for the reaction to occur is characterized by the differential cross-section $\sigma/E'_a, \varphi/$, where φ denotes the angle between the incident beam direction and the direction of the emitted particle b.

This particle has an initial energy E_b according to equation /8/. Traversing the path BC, a further energy loss occurs which is governed by the stopping power $S_b/E/$, so the particle leaves the target surface with energy E_b'. Additional external absorbers can further reduce the energy of the particle before it enters the detector. If the effective thickness of the detector is greater than the range of the particle in the detector material, the particle loses all its energy and the output signal from the detector will be proportional to the particle energy. If, however, the detector is not enough thick to stop the particles the output signal is characteristic of the energy loss of the particle in the detector. By proper choice of the detector thickness and the external absorbers the detecting system can be optimized to detect the wanted reaction product group as background free as possible [14] .

From the wide variety of possible nuclear reactions we restrict ourself to the /d,p/ reactions since these are especially suitable for determining the main light constituents of organic materials because of their high Q-values [6] . A description of the utilization of these A/d,p/B type nuclear reactions in determining the nitrogen and carbon content of organic samples is given with experimental details in ref. [14], again we only summarize the main features of the method.

For nitrogen determination the $^{14}N/d,p_o/^{15}N$ reaction was chosen. The Q-value of this reaction is 8.609 MeV [6] . In choosing the optimal bombarding energy different view-points must be considered: Fig.6 helps us to clarify the situation. The differential cross-sections for this reaction were measured earlier by several groups [15] . Their results at 160^o are displayed in Fig.6/a. On the smoothly increasing cross-section curve a broad peak at 2 MeV deuteron energy is superimposed. This behaviour suggests the use of deuterons of 2 MeV or greater than 4 MeV energy. From Fig.6/b. it can also be seen that the higher the bombarding energy the thicker the sample layer that can be analysed. The energy of the protons leading to the ground state of ^{15}N vs. the projectile energy is shown in Fig. 6/c as calculated by equation /8/. Taking into account this curve the higher bombarding energy is again favoured.

On the other hand in the case of higher bombarding energy the final proton spectrum will be wider due to the increased energy loss of protons coming from deeper sample layers. This broadening could cause difficulties in avoiding interferences from other nuclear reactions. Disturbing proton peaks could come for instance from /d,p/ reactions on ^{10}B, ^{25}Mg, ^{29}Si and ^{33}S isotopes [16] ; for biological samples the silicon isotope seems to be the most troublesome. The overall neutron-dose in the vicinity of the target chamber is also higher with increasing deuteron energy. As a compromise deuterons of 2 MeV energy were generally used in our works. Proton spectra of ammonium nitrate, graphite and cornflour measured in the way described in the experimental part of the paper are shown in Fig.7. The well separated peak at the high energy side of the spectra corresponds to the ground state proton group in the $^{14}N/d,p/^{15}N$ reaction. /In the case of graphite the peak probably originates from adsorbed nitrogen./ The shoulder in the lower energy part of the cornflour and graphite spectra is the result of the $^{13}C/d,p_o/^{14}C$ reaction. In principle this peak could be useful for simultaneous carbon determination. The carbon content is proportional to the dry quantity of the sample, its simultaneous measurement can provide a good basis for data normalization. Series of measurements have confirmed that the reaction chosen is suitable for rapid a few minutes nitrogen determination with high precision /~ 1%/. Separate or simultaneous PIXE measurements allow us to perform elemental analyses correlated to the nitrogen content of the samples.

Experimental

The proton or deuteron beam of 2 MeV energy was generated with the 5 MV Van de Graaff accelerator of the Central Research Institute for Physics. Figure 8 shows the scheme of the target and detector arrangement. An Al diffuser foil of 0.24 mg/cm² thickness was mounted on a 4 mm diameter slit at some distance from the target so as to make the beam profile more uniform. The energy loss of 2 MeV protons and 2 MeV deuterons in this foil are 23 and 42 keV, respectively, but they can easily be compensated for by slightly increasing the primary beam energy. The final beam

definition was performed by a slit of 2 mm diameter positioned only 12 cm from the sample, so the beam spot on the target had a diameter of about 2 mm. Beam currents were only a few nA to avoid deadtime difficulties in the electronics and to prevent the samples from radiation damage. The target chamber was a stainless-steel block with circular holes in all its sides and two other holes for the particle detectors at angles $\pm 160^{o}$ with respect to the incident beam direction. The chamber contained only one sample at a time but a special target changer vacuum lock-system enabled the samples to be quickly changed without disturbing the high vacuum of about 10^{-6} bar produced by a turbomolecular pump. The chamber was insulated from the tube so that it behaved as a Faraday cup, the incoming charges were integrated by an ORTEC Model 439 digital current integrator and counted by a scaler. The X-rays produced passed through the 4 /um Mylar window of the chamber and 11 mm air before entering the CANBERRA Si/Li/X-ray detector through the 25 /um thick Be detector window. The vertical dipstick-type detector was positioned under the chamber at 90^{o} to the incident beam direction. An additional external polypropylene absorber of 25 /um thickness was always used to prevent the scattered protons reaching the detector, otherwise the energetic protons/deuterons/ could lead to a deterioration in the energy resolution and cause a considerable background in the higher energy region. In the case of thick insulating targets the charging up of the sample attracts electrons and the associated bremsstrahlung can destroy the resolution of the system. To prevent charging of the target an electron-emitting hot carbon filament was used [17] . The pulses of the detector were amplified and shaped by CANBERRA X-ray pulse processor electronics and stored via a mixer-router unit in one quarter of the CANBERRA 8100 multichannel analyser. The energy resolution of the system was 175 eV for the 5.89 keV Mn K_{α} line.

The high energy protons from the $^{14}N/d,p/^{15}N$ nuclear reaction were detected by a CsI/Tl/ scintillation detector. The backscattered deuterons and low energy protons were cut off by a 60 mg/cm^{2} Al absorber. The pulses of the particle detector were amplified and shaped by conventional

electronics and also fed into another quarter of the multichannel analyer.

The net peak areas from the spectra were extracted by an off-line TPA-i small computer or, in the case of the particle spectra, by using the digital integration ability of the multichannel analyser. To find the optimal windows for the integrations separate calibrating runs were made with an ammonium nitrate target.

Sample preparation

One of the most critical points in every chemical analysis is the preparation of the sample. Nuclear reaction and PIXE methods can work even in the simplest case too, when direct bombardment of a specimen is performed and no special target preparation is needed. The analysis of single human hairs is an example for this situation. Another possibility is to make pellets from the material to be analysed if sufficient amount of it /few mg/ is available. The drawbacks in both cases are the lower sensitivity and the less accurate evaluation as a consequence of the thickness of the samples. These difficulties are mainly with the PIXE method; the proton spectrum of the nuclear reaction of high Q value used for nitrogen determination is less sensitive to the target thickness.

In most cases, however, thin targets are necessary. In preparing thin targets the material to be analysed is deposited on some suitable backing. There is a wide choice of backing materials /Mylar, carbon, Formvar foil, etc./, and a variety of methods for deposition [18] . The proper choice of the backing material and the deposition method always depend on the specific analytical problem concerned.

Applications

a./ Analysis of superoxide dismutase /SOD/ from the alga 'Anacystis nidulans'.

The SOD enzyme plays an essential role in the protection mechanism of

cells against the toxicity of the O_2^- radical. SOD enzymes of different origin can contain Cu,Zn,Mn or Fe ions as their active centre [19] , for any specific SOD molecule it is important to identify its metal ion content.

The extraction of the enzyme and the target preparation are described elsewhere [19] . Figure 9 shows a PIXE spectrum obtained by proton bombardment of 2 MeV energy, in which only Fe K_α and K_β radiation can be identified /calcium and chlorine peaks are due to the buffer/. This result proves that the SOD of Anacystis nidulans is an iron--containing enzyme. With the help of a separate run of deuteron bombardment the nitrogen content was also determined. The calibration was made by comparing the nitrogen yield with that from the NH_4NO_3 target. The calibration was further checked by independent protein determination by the universally accepted Lowry method. Assuming one iron ion per enzyme molecule the molecular weight of the enzyme could be determined from the quantitative results. The calculations yielded the value of 38000 ± 8000 dalton, being in good agreement with the results obtained by other methods [19] .

b./ Study of binding property of an organic dye.

The dye ZnI_2 OsO_4/ZnIO/ is used to stain the synaptic area of nerve cells. According to earlier ideas the binding was thought to place between the sulphur atoms of amino acids and the dye molecules. To check this idea PIXE-RP measurements were performed on stained glutation and cystein samples. The number of nitrogen atoms in glutation turned out to be three times more than that in cystein, this result is in good agreement with the chemical composition involved. Because both amino acid molecules contain one sulphur atom, equal amounts of Zn, I and Os were expected to belong to the same numbers of the two different amino acid molecules. Contrary to this expectation, many more Zn, I and Os atoms bound to glutation molecules were found suggesting that the amino acid molecules as a whole take part in binding the dye rather than their single sulphur atom alone.

c./ Elemental analysis of single human scalp hairs.

Human scalp hair has long since been recognized as a suitable means for monitoring the variations in the "trace element household" governed by metabolic processes as well as the effect of external contaminations caused by environmental exposure. The concentration variations along a single hair are able to reflect the time dependence of certain elemental concentrations. From the technical point of view, however, it is quite difficult to normalize the quantities of different trace elements. To find a proper normalization method PIXE-RP measurements were carried out along single hairs of different donors [20] . The plucked hairs themselves were directly bombarded by 2 MeV deuterons. The main results are displayed in Fig.10. The S/N and S/C ratios are fairly constant along the whole hair indicating that the quantity of sulphur represents the analysed amount of hair in the same manner as that of carbon or nitrogen. Utilizing this result the quantities of elements of higher atomic number determined by proton induced X-rays can be normalized to sulphur content measured simultaneously at the same hair volume element. Calcium or even zinc concentrations determined in this way show significant variations along the length of a hair. The result for Zn is particularly interesting because earlier the amount of Zn was considered to be a suitable candidate for performing normalizations [21] .

Summary

The combination of the PIXE method and the $^{14}N/d,p/^{15}N$ nuclear reaction allows simultaneous trace element and nitrogen content determination. With the help of this latter item of data it is possible to relate the concentrations determined by PIXE to the protein content of the sample. During some ten minutes, trace element contributions in the ppm range can be determined with a statistical accuracy of almost ten per cent. Usually very small amount of material is sufficient for the measurement, so there is the possibility to follow a certain element in the successive

steps of a biochemical separation process. In this way, in addition to the quantities of certain elements, sometimes conclusions can be drawn about their binding place, which could provide useful information to understand the functional role of the elements of interest.

References

[1] Johansson, S.A.E., and Johansson, T.B. /1976/ Nucl. Instr. Meth. 137, 473
Deconninck, G., Demortier, G., and Bodart, F. /1975/ Atomic Energy Review 13, 367

[2] Rhodes, J.R. /1971/ in "Energy Dispersion X-Ray Analysis: X-Ray and Electron Probe Analysis" /Russ, J.D. ed./ ASTM SPT. 485, 243

[3] "Microprobe Analysis as Applied to Cells and Tissues" /1974/ /Hall, T., Echlin, P., and Kaufmann, R., eds./ Academic Press, New York.

[4] Woldseth, R. /1973/ "X-Ray Energy Spectrometry" Kevex Corp. Burlingame.

[5] FAO, Rome /1970/ Nutritional Studies No.24

[6] Deconninck,G. /1978/ "Introduction to Radioanalytical Physics" Elsevier, Amsterdam - Akadémiai Kiadó, Budapest.

[7] Bambynek, W., Crasemann, B., Fink, R.W., Freund, H.U., Mark, H., Swift, C.D., Price, R.E., and Venugopala Rao, P. /1972/ Rev. Mod. Phys. 44, 716

[8] Folkmann, F. /1976/ in "Ion Beam Surface Layer Analysis" /Meyer, O., Linker, G., and Käppeler, F., eds./ Vol.2, pp. 747 Plenum Press, New York

[9] Shima, K., Makino, I., and Sakisaka, M. /1971/ J.Phys.Soc.Jap. 30, 611
Singh, B. /1957/ Phys.Rev. 107, 711

[10] Szőkefalvi-Nagy, Z., and Demeter, I., /1981/ Nucl.Instr.Meth.

[11] Storm, E., and Israel, H.I. /1970/ Nucl. Data. A7, 565
McMaster, W.H., Kerr Del Grande, N., Mallett, J.H., and Hubbel, J.H. /1969/ UCRL-50174. Rev.1.
Veigele, J. /1973/ Atomic Data 5, 66

[12] Northcliffe, L.C., and Schilling,R.F. /1970/ Nucl.Data A7, 233
Williamson, C.F., Boujot, J.P., and Picard, J. /1966/ Repport CEA-R 3042.

[13] Demeter,I., Keszthelyi, L., Szőkefalvi-Nagy, Z., Varga, L., Hollós-Nagy, K., and Nagy, Á. /1979/ Acta Biochim. et Biophys. Acad. Sci. Hung. 14, 189

[14] Varga, L. /1977/ Report 102. KFKI.

[15] Gallmann, A., Fintz, P., and Hodgson, P.E. /1966/ Nucl.Phys. 82, 161
Beaumevieille, H., Lambert, M., Yaker, M. and Amokvone, A. /1967/ Il Nuovo Cimento XLVIIB. 139
Kawai, N. /1961/ J.Phys.Soc.Jap. 16, 157

[16] Olivier, C., and Peisach, M. /1972/ J.Radioanal.Chem. 12, 313

[17] Ahlberg, M., Johansson, G., and Malmquist, M. /1976/ Nucl. Instr. Meth. 131, 377

[18] Campbell, J.L. /1977/ Nucl. Instr. Meth. 142, 263

[19] Cséke, Cs., Horváth, L.I., Simon, P., Borbély, G., Keszthelyi, L., and Farkas, G. /1979/ J.Biochem. 85, 1397
Demeter, I., Keszthelyi, L., Szőkefalvi-Nagy, Z., Varga, L., and Hollós-Nagy, K. /1979/ Acta Biochem. et Biophys. Acad. Sci. Hung. 14, 197

[20] Varga, L., Szőkefalvi-Nagy, Z., Demeter, I., Bódi, T. /1980/ Acta Biochim. et Biophys. Acad. Sci. Hung. 15, 132

[21] Report of the Advisory Group on "Accelerator-Based Techniques for the Analysis of Trace Element Pollutants in Man", IAEA, Vienna, 23 - 26 January 1978. /unpublished/

Figure captions

Fig. 1 Experimental K and L shell ionization cross-sections for proton impact [1] , U_i/i=K or L/ means the electron binding energy in the K or L shell, E is the proton energy and λ the ratio of the proton mass to the electron mass. The solid lines are the semiempirical functions proposed in ref. [1] .

Fig. 2 Production cross-sections of K and L X-rays induced by 2 MeV protons and the efficiency curve for a commercial Si/Li/ X-ray detector vs. X-ray energies.

Fig. 3 Proton excited X-ray spectrum of cholinergic presynaptic vesicles prepared from guinea-pig brain cortex [13] .

Fig. 4 Minimum detectable concentrations of different chemical elements embedded in thick carbon matrix for bombardment by protons of 2 MeV energy.

Fig. 5 Geometry to measure charged particle reaction products.

Fig. 6 a, Differential cross-sections at 160^{o} for the $^{14}N/d,p_o/^{15}N$ reaction [15] ; b, range of deuterons in thick carbon layer; c, energy of the p_o protons emitted at angle 160^{o} as a function of the energy of the bombarding deuteron beam.

Fig. 7 Proton spectra from ammonium nitrate, pelletized cornflour and graphite targets bombarded by 1.5 MeV deuterons.

Fig. 8 Scheme of the target and detector arrangement.

Fig. 9 PIXE spectrum of superoxide dismutase prepared from alga 'Anacystis nidulans'.

Fig.10 The S/N, S/C and Ca/S peak intensity ratios measured along a single hair, the indicated distance is measured from the hair root.

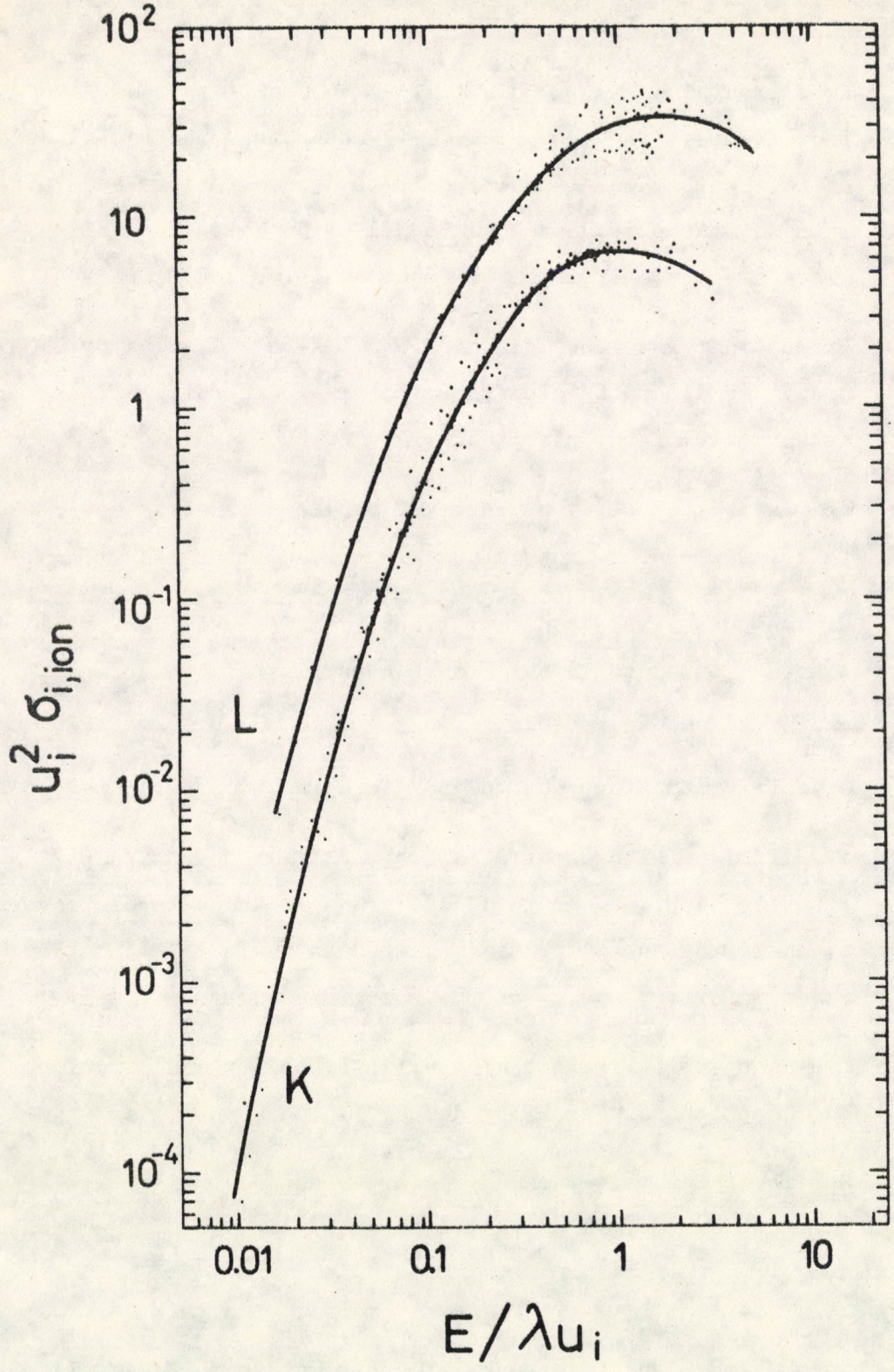

Figure 1

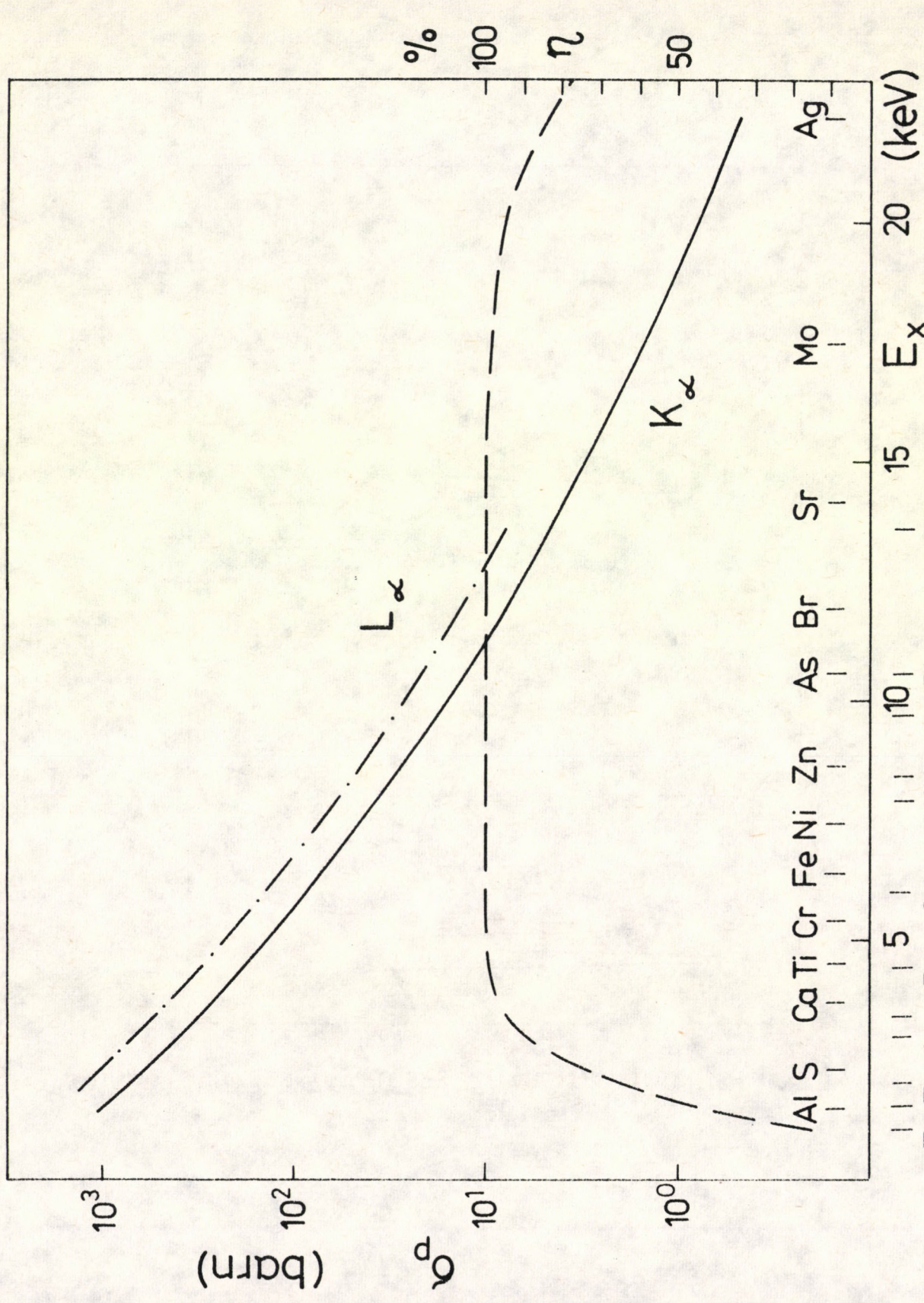
% 100 η 50
Ag
20 (keV)
Mo
15 E_x
Sr
U
As Br
10
Au Pb
Hf W
Zn
Fe Ni
Cr
Ti
Ca
5
S
Al
Zn Zr Ag Ba Gd
L_α
K_α
10^3
10^2
10^1
10^0
σ_p (barn)

Figure 2

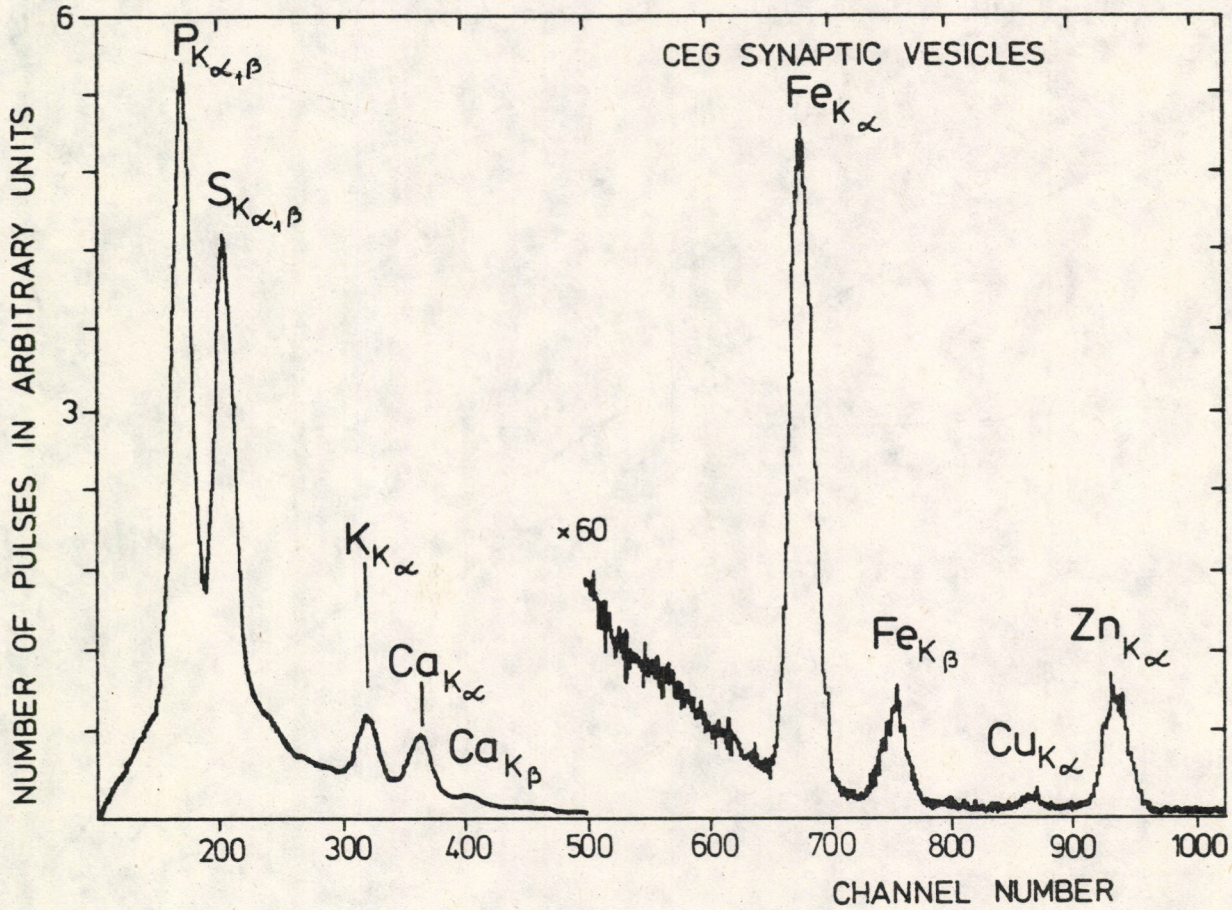
CEG SYNAPTIC VESICLES
NUMBER OF PULSES IN ARBITRARY UNITS
CHANNEL NUMBER
6
3
200
300
400
500
600
700
800
900
1000
$P_{K\alpha_{1,\beta}}$
$S_{K\alpha_{1,\beta}}$
$K_{K\alpha}$
$Ca_{K\alpha}$
$Ca_{K\beta}$
×60
$Fe_{K\alpha}$
$Fe_{K\beta}$
$Cu_{K\alpha}$
$Zn_{K\alpha}$

Figure 3

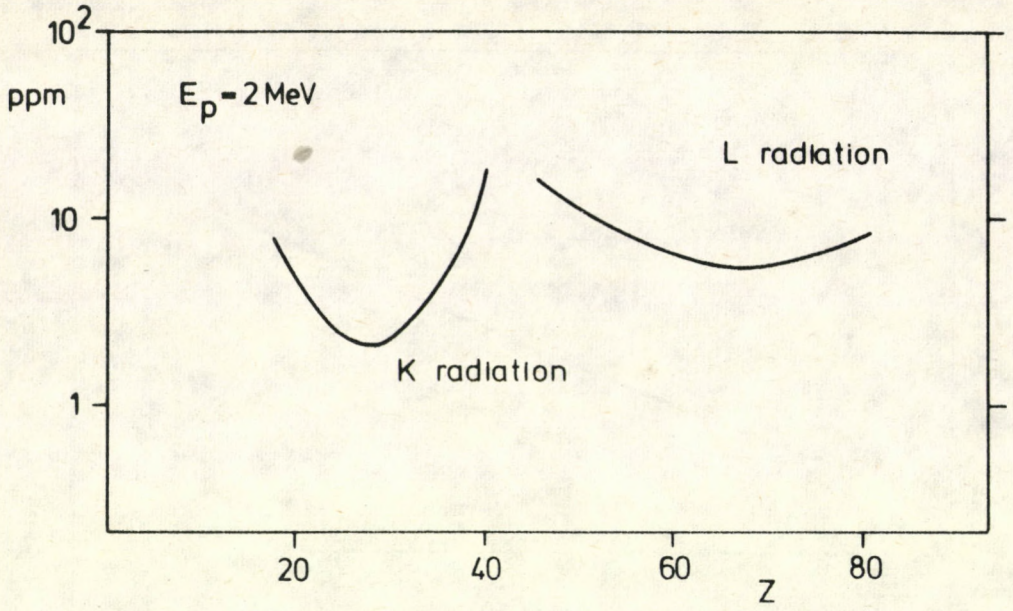

Figure 4

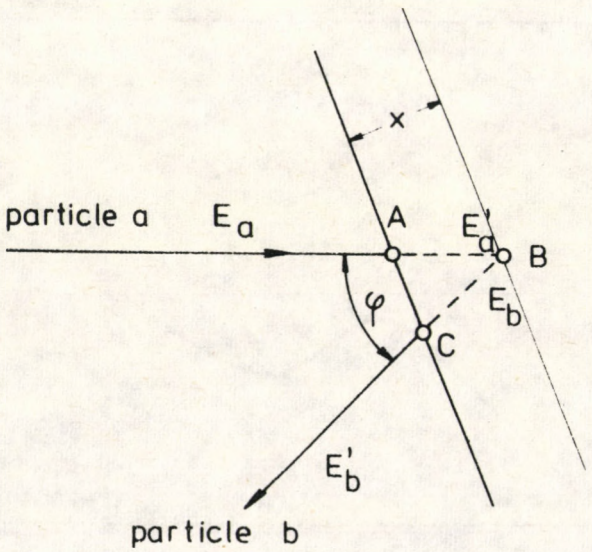

Figure 5

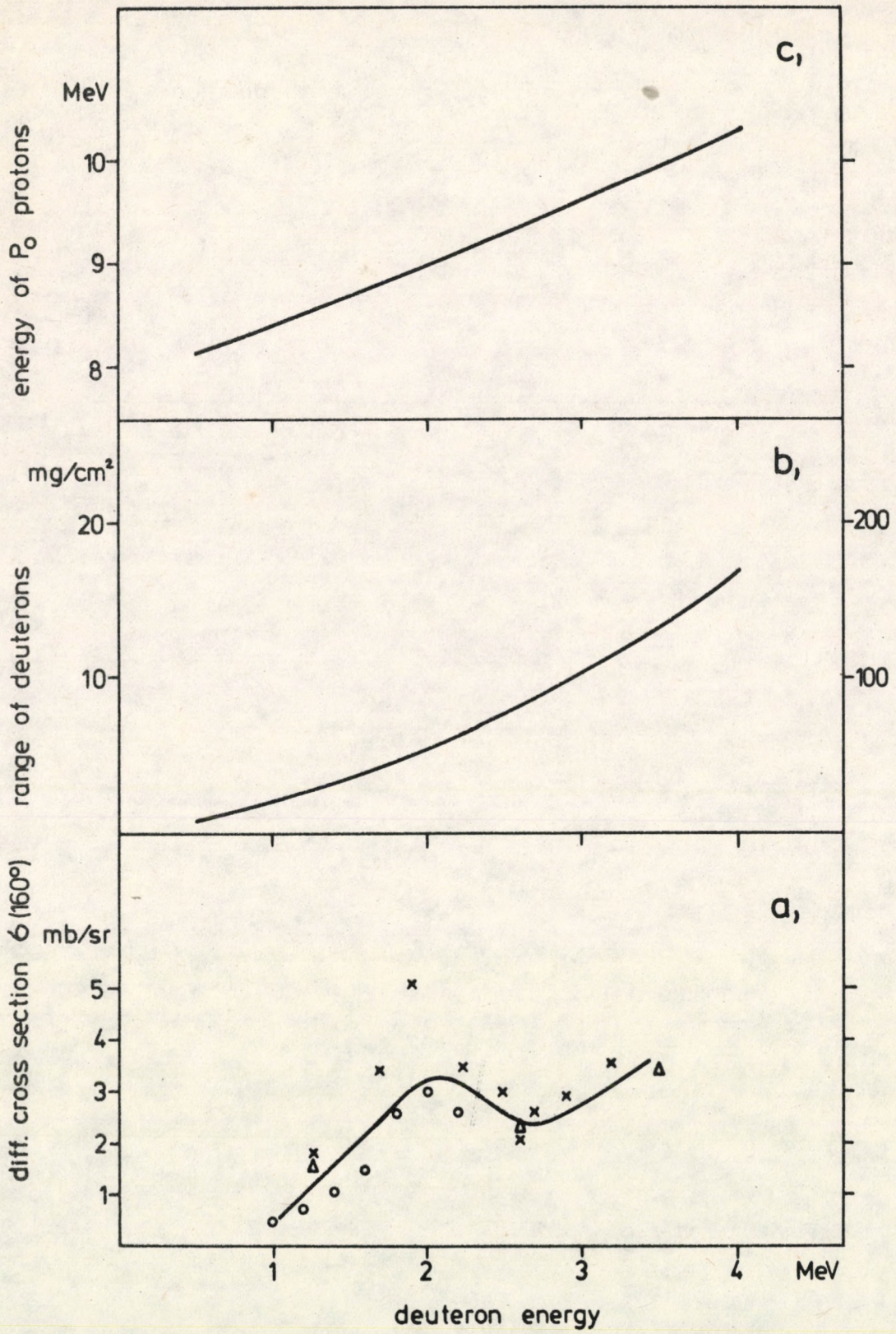
c,
MeV
10
9
8
energy of P_o protons
b,
mg/cm²
20
10
200
100
range of deuterons
a,
mb/sr
5
4
3
2
1
diff. cross section 6 (160°)
1
2
3
4
MeV
deuteron energy

Figure 6

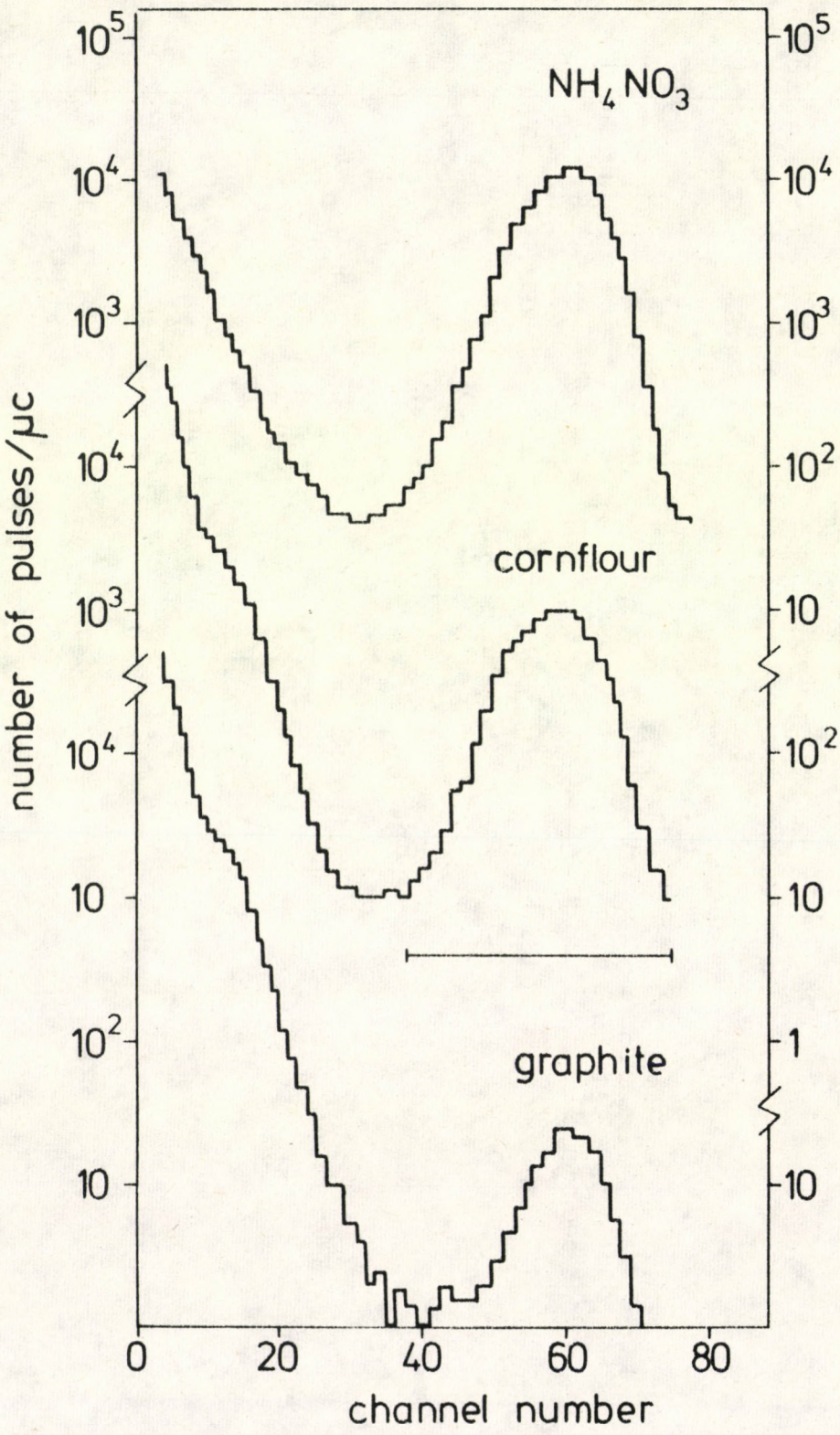
NH_4NO_3
cornflour
graphite
number of pulses/μc
channel number
0
20
40
60
80
10^5
10^4
10^3
10^2
10
1

Figure 7

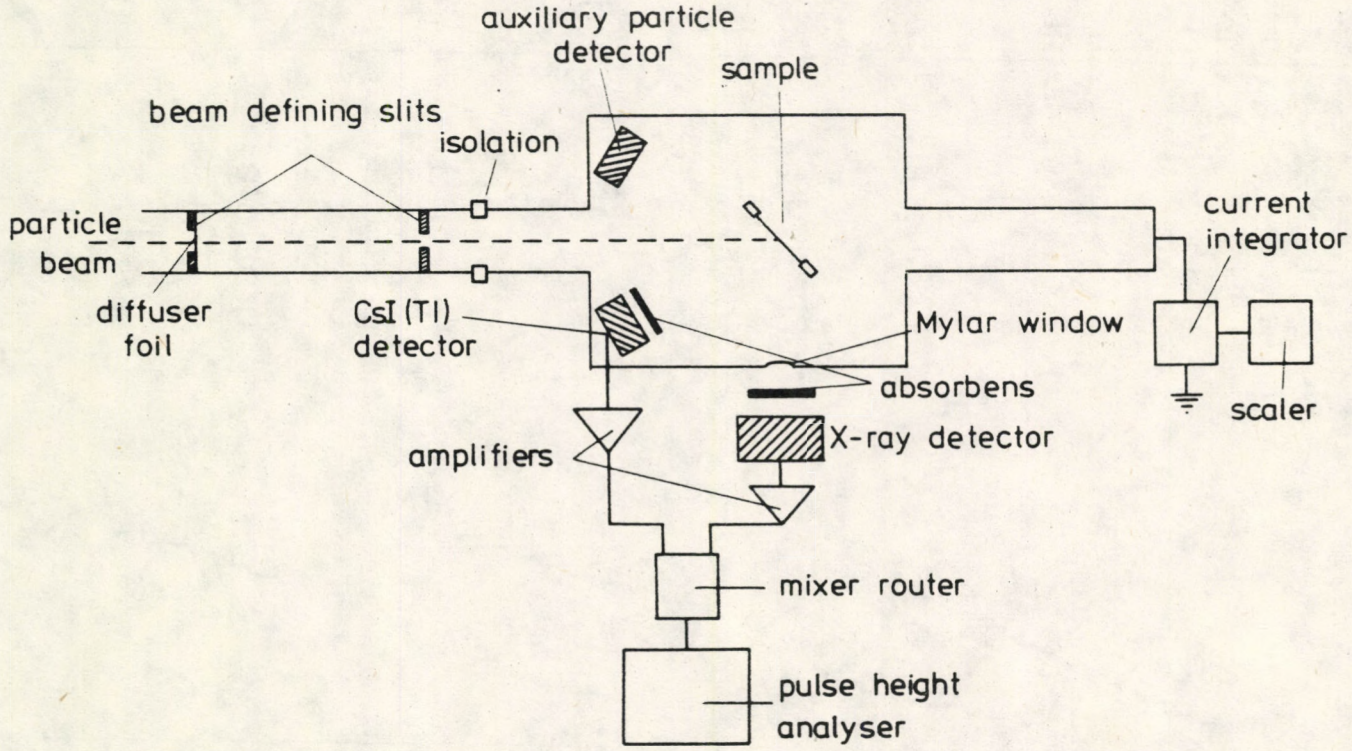
auxiliary particle
detector
sample
beam defining slits
isolation
particle
beam
current
integrator
diffuser
foil
CsI (Tl)
detector
Mylar window
absorbens
scaler
amplifiers
X-ray detector
mixer router
pulse height
analyser

Figure 8

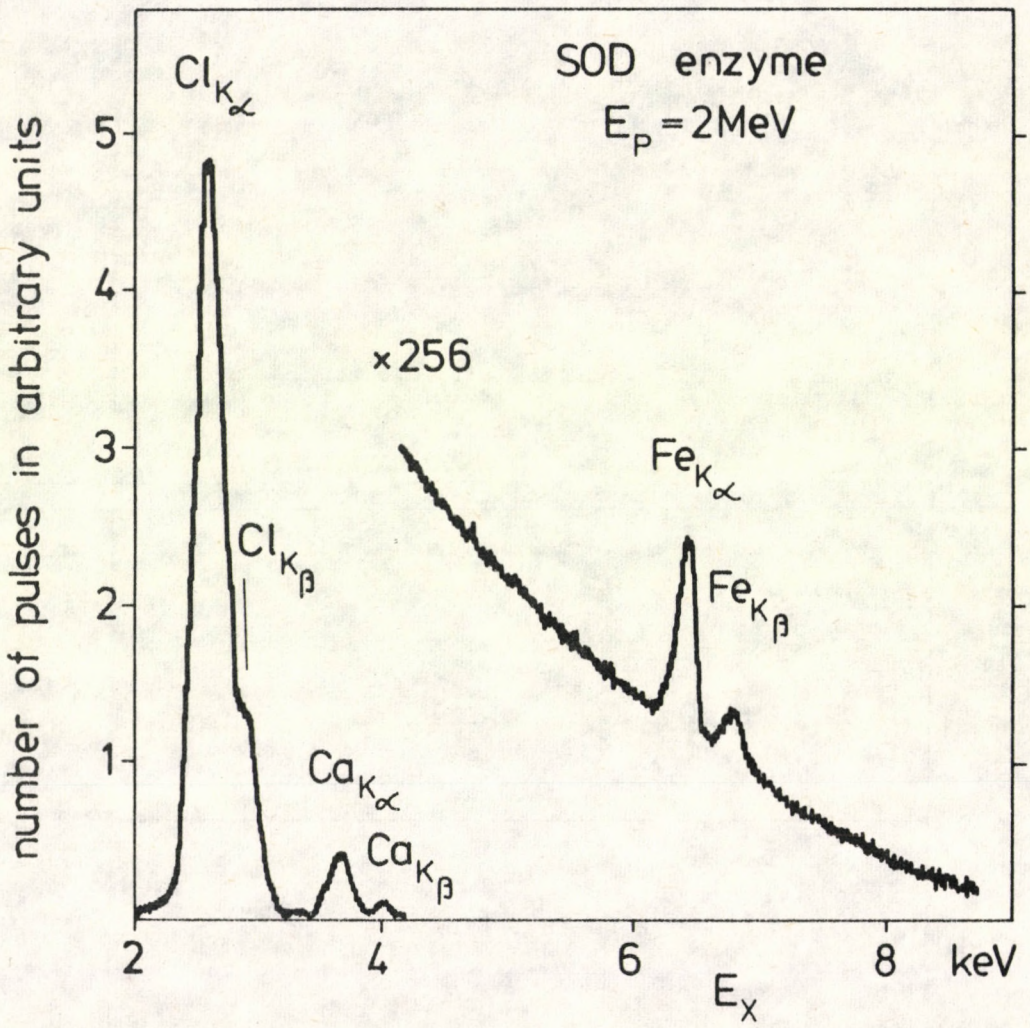
SOD enzyme
$E_p = 2MeV$
$Cl_{K\alpha}$
$Cl_{K\beta}$
$Ca_{K\alpha}$
$Ca_{K\beta}$
×256
$Fe_{K\alpha}$
$Fe_{K\beta}$
number of pulses in arbitrary units
1
2
3
4
5
2
4
6
8
keV
E_X

Figure 9

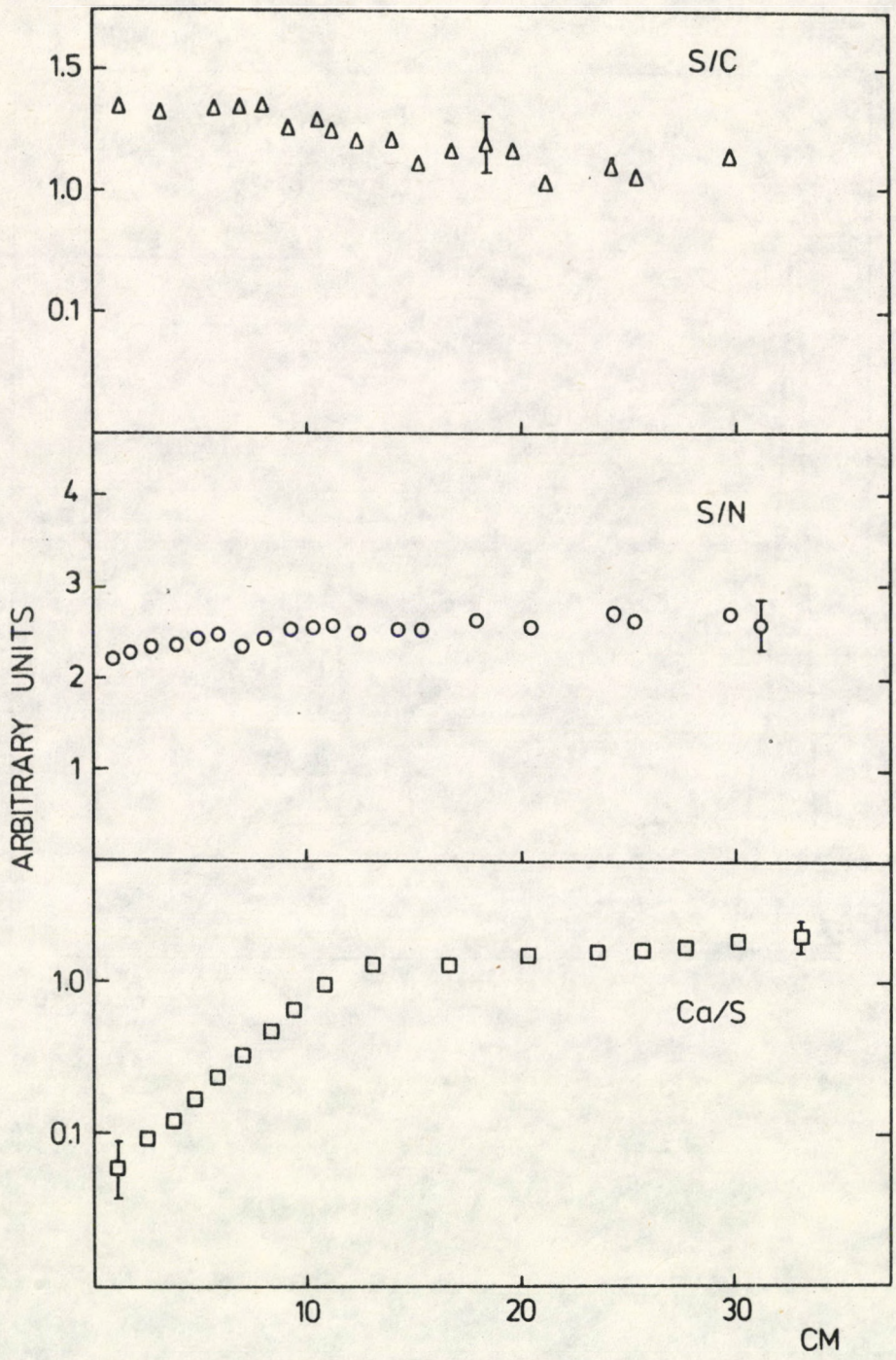

Figure 10

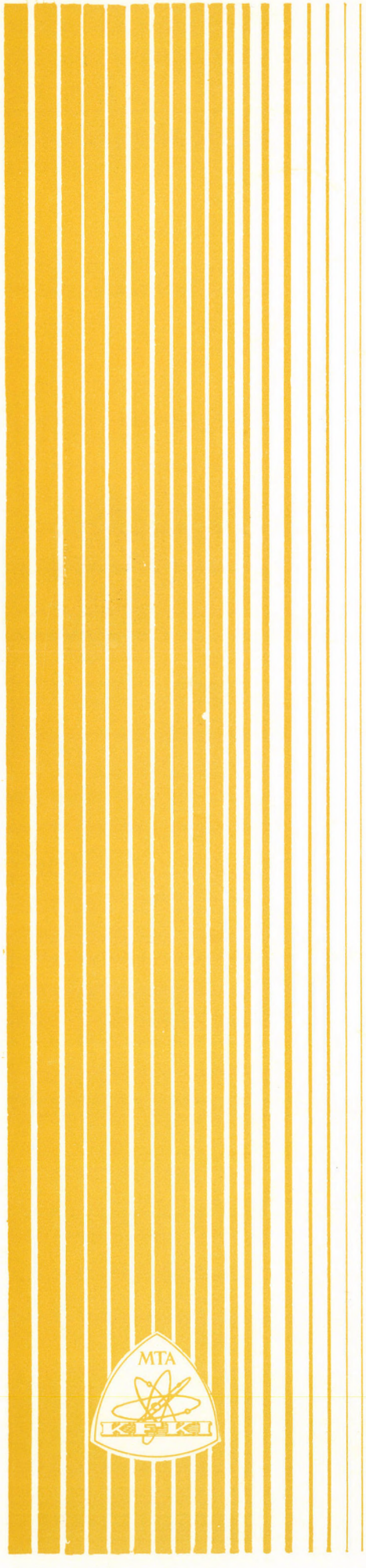

Kiadja a Központi Fizikai Kutató Intézet
Felelős kiadó: Szegő Károly
Szakmai lektor: Lohner Tivadar
Nyelvi lektor: Harvey Shenker
Példányszám: 370 Törzsszám: 81-235
Készült a KFKI sokszorosító üzemében
Felelős vezető: Nagy Károly
Budapest, 1981. április hó